

# 1 Supplementary material for LHCb-PAPER-2018-004

2 Figure 1 shows the neural network response of simulated  $\bar{B}^0 \rightarrow \bar{K}^{*0} \mu^+ \mu^-$  decays and of  
3 candidates with  $m(K^- \pi^+ \mu^+ \mu^-) > 5670 \text{ MeV}/c^2$ . Figure 2 shows the  $q^2$  and  $m(K^- \pi^+)$   
4 distribution of the  $B_s^0 \rightarrow \bar{K}^{*0} \mu^+ \mu^-$  candidates, where a background subtraction has  
5 been carried out using the *sPlot* technique [1]. The  $B_s^0 \rightarrow \bar{K}^{*0} \mu^+ \mu^-$  decay accounts for  
6 approximately 60% of the candidates in this mass region. The remaining candidates  
7 comprise a mixture of  $B^0 \rightarrow \bar{K}^{*0} \mu^+ \mu^-$  decays, combinatorial and specific backgrounds.  
8 Figure 3 combines the different data taking periods and neural network response bins.  
9 In the combination, the candidates are weighted by the  $B_s^0 \rightarrow \bar{K}^{*0} \mu^+ \mu^-$  signal purity  
10 as suggested in Ref. [2]. The signal purity is defined as  $N_S/(N_S + N_B)$ , where  $N_S$  is the  
11 expected  $B_s^0 \rightarrow \bar{K}^{*0} \mu^+ \mu^-$  yield in each category based on the result of the simultaneous  
12 fit and  $N_B$  is the background yield in that category. Both  $N_S$  and  $N_B$  are determined  
13 within  $15 \text{ MeV}/c^2$  of the  $B_s^0$  peak position. The uncertainty on the data points in Fig. 3 is  
14 given by the sum of the weights squared.

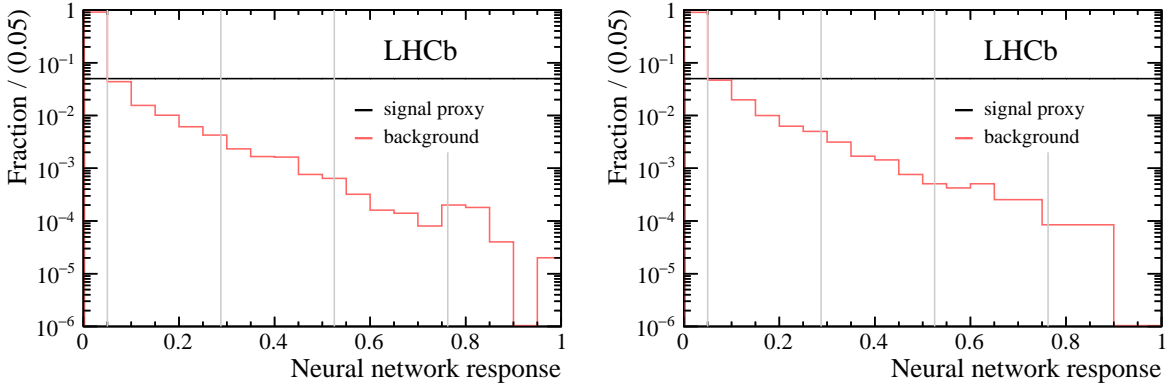


Figure 1: Neural network response of (left) simulated  $\bar{B}^0 \rightarrow \bar{K}^{*0} \mu^+ \mu^-$  decays and candidates with  $m(K^- \pi^+ \mu^+ \mu^-) > 5670 \text{ MeV}/c^2$  in the Run 1 data set and (right) simulated  $\bar{B}^0 \rightarrow \bar{K}^{*0} \mu^+ \mu^-$  decays and candidates with  $m(K^- \pi^+ \mu^+ \mu^-) > 5670 \text{ MeV}/c^2$  in the Run 2 data set. The neural network response is calibrated to be uniform for the simulated  $\bar{B}^0 \rightarrow \bar{K}^{*0} \mu^+ \mu^-$  decays. Candidates with a neural network response below 0.05 are rejected in the analysis. The vertical lines indicate the boundaries of the four bins of neural network response used in the fit.

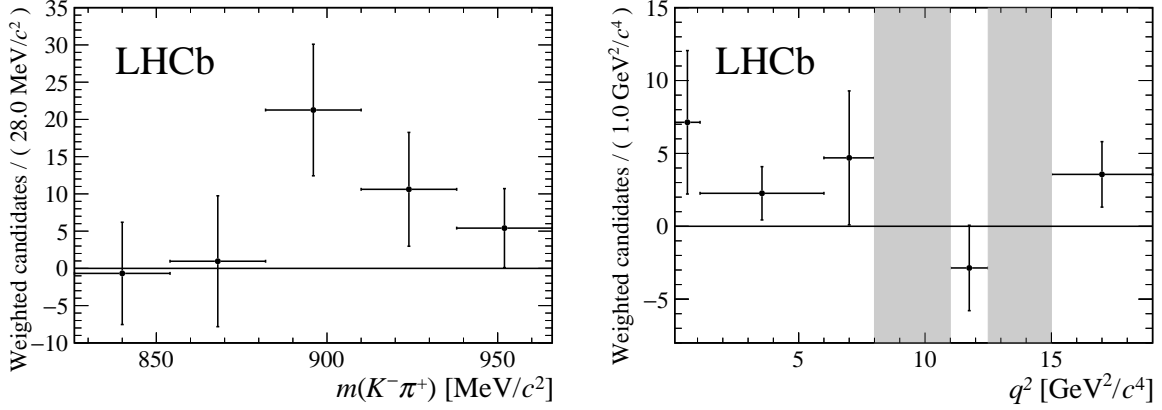


Figure 2: Distribution of reconstructed  $K^-\pi^+$  invariant mass and  $q^2$ -value of background subtracted candidates. Candidates with  $8.0 < q^2 < 11.0 \text{ GeV}^2/c^4$  and  $12.5 < q^2 < 15.0 \text{ GeV}^2/c^4$  have been removed to reject decays via intermediate  $J/\psi$  and  $\psi(2S)$  resonances.

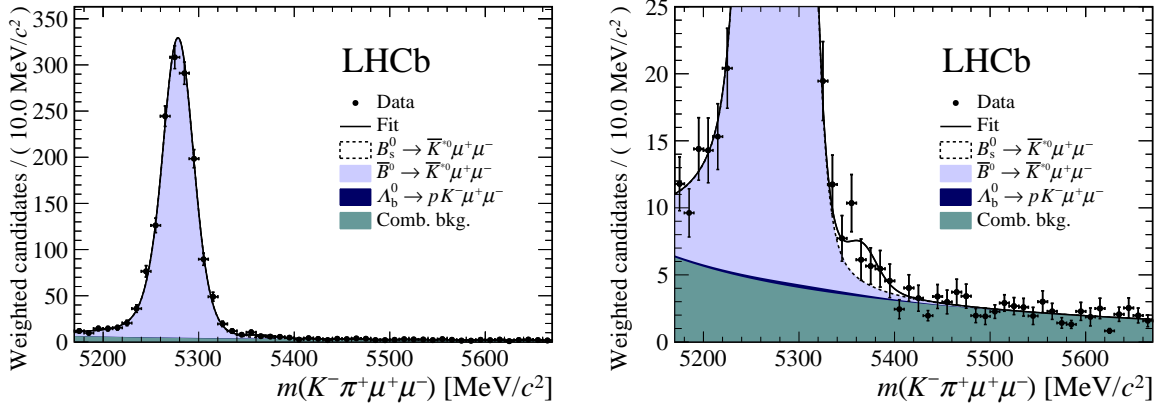


Figure 3: The  $K^-\pi^+\mu^+\mu^-$  invariant mass weighted by signal purity of the candidates combined over all neural network bins, shown (left) over the full range and (right) over a restricted vertical range to emphasise the  $B_s^0 \rightarrow \bar{K}^{*0}\mu^+\mu^-$  component. The line indicates a combination of the results of the fits to the individual bins, also weighted by signal purity. Components are detailed in the legend, where they are shown in the same order as they are stacked in the figure.

## 15 **References**

16 [1] M. Pivk and F. R. Le Diberder, *sPlot: A statistical tool to unfold data distributions*,  
17 Nucl. Instrum. Meth. **A555** (2005) 356, [arXiv:physics/0402083](#).

18 [2] R. J. Barlow, *Event classification using weighting methods*, J. Comput. Phys. **72** (1987)  
19 202.